Rare Metal Materials and Engineering
Volume 53, Issue 2, February 2024
Available online at www.rmme.ac.cn

Science Press

Cite this article as: Li Jiangtao, Luo Yongjin, Su Zhun, et al. Preparation of Ultrafine Nanosized Tungsten Carbide by Hydrothermal Synthesis of Tungsten Precursor, Carbothermic Reduction, and Carburization[J]. Rare Metal Materials and Engineering, 2024, 53(02): 321-329. DOI: 10.12442/j.issn.1002-185X.E20230018.

ARTICLE

Preparation of Ultrafine Nanosized Tungsten Carbide by Hydrothermal Synthesis of Tungsten Precursor, Carbothermic Reduction, and Carburization

Li Jiangtao[1,2], Luo Yongjin[1], Su Zhun[1,3], Zhao Zhongwei[1,2], Chen Ailiang[1], Liu Xuheng[1], He Lihua[1,2], Sun Fenglong[1], Chen Xingyu[1,2]

[1] School of Metallurgy and Environment, Central South University, Changsha 410083, China; [2] Key Laboratory of Hunan Province for Metallurgy and Material Processing of Rare Metals, Changsha 410083, China; [3] School of Materials Science and Engineering, Shanghai Jiao Tong University, Shanghai 200240, China

Abstract: A novel method to prepare ultrafine WC was proposed: the $PbWO_4$ prepared by hydrothermal synthesis was used as raw material, and WC was obtained through the carbothermic reduction-carburization process. $PbWO_4$ was used as the tungsten intermediate product to avoid the introduction of ammonia nitrogen reagent. The carbon reduction method can avoid the generation of water vapor and inhibit the growth of tungsten powder. Results show that more than 99.9wt% of W is extracted in the form of $PbWO_4$ from the Na_2WO_4 solution under the conditions of initial pH value of 7.0, reaction temperature of 160 °C, and reaction time of 4.5 h. Then, the homogeneous mixture of W and C is obtained by the carbothermic reduction of $PbWO_4$ at 950 °C for 3 h with the molar ratio of carbon:tungsten as 5. Pre-adding excessive carbon in the mixture can inhibit the agglomeration of tungsten powder. Subsequently, the WC powder with particle size of about 60 nm is obtained by the carburization of the W and C mixture at 1200 °C for 6 h.

Key words: $PbWO_4$; ultrafine WC; hydrothermal method; reductive carbonization

Tungsten is an important strategic metal to produce cemented tungsten carbides (WC)[1]. The mechanical properties of cemented carbides strongly depend on the grain size of WC[2–3]. Dissimilar to traditional cemented carbides, ultrafine cemented carbides can simultaneously improve the hardness and toughness, comprehensively enhancing the brittleness and machining softening[4–5]. Therefore, the development of ultrafine-grained cemented carbides and nanocrystalline microstructures attracts much attention. However, technical difficulties restrict the preparation of ultrafine cemented carbides[6], such as the preparation of high-quality ultrafine WC raw material and the strict conditions of grain length and coarseness of ultrafine cemented carbide during sintering.

With the development of modern technique, the particle size is refined from 0.2 μm to 0.1 μm (BET measurement value) in the industrial production of ultrafine WC powders[7]. The industrial route to prepare ultrafine WC powders involves the following reactions[8]: tungsten concentrate→Na_2WO_4→$(NH_4)_2WO_4$→ammonium paratungstate (APT) →WO_x→W powder→ultrafine WC powder. Tungsten concentrate, especially scheelite, is usually consumed through soda autoclaving process and caustic soda autoclaving process[9]. Soda autoclaving is mainly used in western countries, whereas caustic soda autoclaving is more commonly used in China[10]. Because intermediate products, such as APT, are inevitably produced in the tungsten metallurgy, ammonia nitrogen wastewater is generated during the ion exchange or solvent extraction, which contains a large number of non-ferrous metals[11]. In addition, during the preparation of W powder by the hydrogen reduction of WO_x, H_2O will react with fine tungsten powder to form $WO_2(OH)_2$ gas, which then reacts

Received date: July 05, 2023
Foundation item: National Natural Science Foundation of China (51334008); National Key Research and Development Program of China (2022YFC2904505); Project of Basic Science Center of the National Natural Science Foundation (72088101)
Corresponding author: Chen Xingyu, Ph. D., Professor, School of Metallurgy and Environment, Central South University, Changsha 410083, P. R. China, E-mail: xychen@csu.edu.cn

with H_2 to produce large tungsten powder particles[12–13]. In industry production, the growth of tungsten particles can be inhibited by decreasing the reduction temperature, providing hydrogen flow, or reducing the thickness of material layer[14–15]. However, these methods do not inherently prevent water production, and the resultant tungsten particles are still larger than 100 nm in size[16].

Currently, many methods are proposed to prepare tungsten carbide powder. Among them, mechanical alloying is a simple technique to produce ultrafine WC powder. Razavi et al[17] used W and carbon black as raw materials and added a small amount of WC into the mixture. Under the protection of argon, WC nanopowder with particle size of 8–69 nm was obtained by high-energy ball milling. However, this carbonization process has long duration of 75–150 h, which causes more energy consumption and introduces more pollution sources. Chemical vapor synthesis accelerates the carbonization process and produces ultrafine WC powder by hydrogen and hydrocarbon vapor reduction precursors, such as WCl_6[18], $W(CO)_6$[19], and WF_6[20]. Although this technique can synthesize ultrafine powders with controllable particle size, shape, and crystal structure, the formation of phase-pure WC powder is still challenging. This is mainly because the carburization reaction process is fast, and the generated intermediate W_2C is difficult to completely transform into WC. Other methods, such as solvothermal method[21–22], combustion synthesis[14,23], wire explosion[24–25], and thermochemical processes[26–27], are also commonly used to produce ultrafine WC powder. Nevertheless, further experiment studies are still required to ameliorate these methods for large-scale industrial application.

There are various problems during the treatment of ammonia nitrogen wastewater in the tungsten metallurgy industry, which makes it difficult to obtain ultrafine tungsten powder via the hydrogen reduction of WO_x. Therefore, in this research, a novel method was proposed to obtain ultrafine WC powder via the hydrothermal synthesis of $PbWO_4$ coupled with carbothermic reduction-carburization process. In this treatment process, tungsten was extracted from sodium tungstate leachate based on the low solubility of $PbWO_4$. Then, based on the highly saturated vapor pressure of lead, $PbWO_4$ was reduced by carbon and then the lead was volatilized as gaseous form, separated from the ultrafine WC powder. To suppress the agglomeration of ultrafine tungsten powder, carbon for WC generation was added before the carbon reduction of WO_x. Thus, the W-C mixed powder was obtained through the carbothermal reduction process. Finally, the W-C mixed powder was carburized at high temperature to obtain ultrafine WC powder.

1 Experiment

All reagents used in this research were of chemical grade and without further purification. $Pb(NO_3)_2$, CH_3CH_2OH, HNO_3, and NaOH were purchased from Sinopharm Group Chemical Reagent Co., Ltd, China. $Na_2WO_4{\cdot}2H_2O$ was purchased from Shanghai Macklin Biochemical Technology Co., Ltd. Carbon black (MA100, 99.5wt% purity) was purchased from Mitsubishi Chemical Corporation.

In the typical hydrothermal synthesis, 100 mL Na_2WO_4 solution containing 100 g/L WO_3 and equimolar concentration of $Pb(NO_3)_2$ solution were prepared. The solutions were mixed and stirred for 30 min. NaOH and HNO_3 solutions were used to adjust the pH value of the mixed solutions during stirring. The as-prepared mixture was transferred to a stainless steel autoclave (500 mL), which was then sealed and hydrothermally treated. The influence of hydrothermal reaction temperature, holding time, and pH value on the hydrothermal products was studied. The precipitate produced during the reaction was washed several times with deionized water and absolute ethanol, and they were dried at 80 °C for 6 h.

The carbothermal reduction-carburization experiment was conducted in a horizontal tube furnace (GSL-1700X, Hefei Kejing Materials Technology Co., Ltd). $PbWO_4$ and carbon black were mechanically mixed in an agate mortar for 20 min. Then, 5.6 g mixed powder was placed in an alumina boat and pushed into the tube furnace for carbon reduction. The specimen was heated to the designed temperature at heating rate of 5 °C/min and held for different durations. After reactions, the specimens were cooled to room temperature, removed from the furnace, and mixed again. Finally, after putting the mixture back into the furnace, the furnace was reheated to a high temperature at heating rate of 5 °C/min to initiate the carburization process. The whole reaction process was conducted under the protection of argon flow (100 mL/min).

The carbothermal reduction process of $PbWO_4$ was studied by non-isothermal experiment using thermogravimetric (TG) analysis/differential scanning caloimetry (DSC) simultaneous thermal analyzer (STA 449 F5 Jupiter, NETZSCH, Germany). The specimen was placed into the analyzer, heated from room temperature to 1200 °C at heating rate of 5 °C/min, and held for 1 h under the protection of argon flow (80 mL/min). The morphology, particle size, and distribution of reaction products were observed through field emission-scanning electron microscope (FE-SEM, CLARA, TESCAN, Czech Republic) and transmission electron microscope (TEM, JEM-F200, JEOL, Japan). The phase composition of reaction products was determined by X-ray diffraction (XRD, Empyrean, PANalytical, Netherlands). The concentration of tungsten in the solution was determined by ICP-OES (ICP 7400, Thermofisher, USA).

2 Results and Discussion

2.1 Extraction of W from Na_2WO_4 solution via hydrothermal synthesis of $PbWO_4$ nanocrystals

2.1.1 Effect of initial pH value of solution

The pH value of Na_2WO_4 solution was adjusted for $PbWO_4$ precipitation. The precipitation effect is shown in Fig. 1a. When pH<7.0, the $PbWO_4$ precipitate yield barely changes and remains at approximately 99.99%. When the pH value is above 7.0, the $PbWO_4$ precipitate yield decreases from 99.99% to 97.64%. According to Fig. 1b, the pH value of solution does not affect the phase composition of hydrothermal products. All diffraction peaks of synthesized

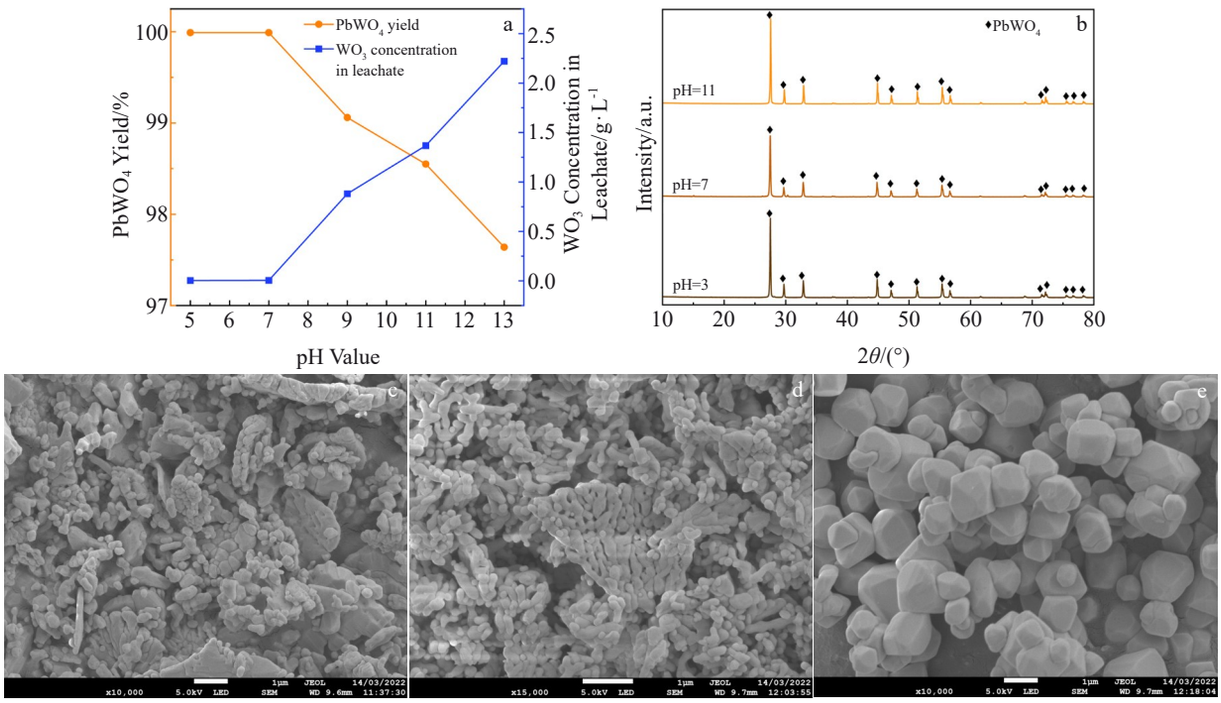

Fig.1 Effect of initial pH value of Na_2WO_4 solution on $PbWO_4$ precipitation at 160 °C for 4.5 h (a); XRD patterns of hydrothermal products prepared at different pH values (b); FE-SEM morphologies of $PbWO_4$ precipitates synthesized at pH=3 (c), pH=7 (d), and pH=11 (e)

products correspond to the pure tetragonal $PbWO_4$ with scheelite structure (JCPDS No. 19-0708). No other crystalline impurities can be detected.

FE-SEM morphologies of $PbWO_4$ nanocrystals are shown in Fig. 1c–1e. When the initial pH value of the solution is 3, the $PbWO_4$ particles have irregular shapes with broad size distribution, as shown in Fig. 1c. Many cracks appear on the surface of large flake particles, indicating the cracking phenomenon. When the initial pH value of the solution is 7, the synthesized $PbWO_4$ nanocrystals still have irregular shapes with many gaps. This result indicates that large $PbWO_4$ particles decompose into small particles with average size of about 0.4 μm. When the initial pH value of the solution is 11, the synthesized $PbWO_4$ particles have regular polyhedral shapes with sharp corners and edges, as shown in Fig. 1e. The average size increases to 1.5 μm. Therefore, the optimal initial pH value of the solution is 7 to obtain ultrafine $PbWO_4$ products.

2.1.2 Effect of temperature

Fig. 2 shows the effect of reaction temperature on the phase and morphology of the hydrothermal products. All diffraction peaks correspond to the pure $PbWO_4$, suggesting that the reaction temperature does not change the phase of the hydrothermal products. The diffraction peak intensity of $PbWO_4$ synthesized at room temperature (25 °C) is significantly weaker, indicating that hydrothermal synthesis improves the crystal quality of $PbWO_4$ particles. When the reaction is conducted at 25 °C, the synthesized $PbWO_4$ particles are irregular with coarse surfaces, as shown in Fig. 2b. Large $PbWO_4$ particles gradually decompose into small particles when the reaction temperature increases to 160 °C. However, when the temperature reaches 180 °C, $PbWO_4$ particles are composed of numerous small agglomerated particles, as shown in Fig. 2e. The average size of small particles is about 0.8 μm. Consequently, 160 °C is the optimal temperature for $PbWO_4$ precipitation.

2.1.3 Effect of reaction duration

Fig. 3 shows the effect of reaction durations on the phase and morphology of the hydrothermal products. Prolonging the reaction duration does not change the phase composition of the hydrothermal products, which are all composed of pure $PbWO_4$. According to Fig. 3b–3c, with prolonging the reaction duration from 1.5 h to 4.5 h, large $PbWO_4$ particles break into small particles. However, when the reaction duration further increases to 7.5 h, the morphology of $PbWO_4$ nanocrystals significantly changes. This is because the Ostwald ripening (dissolution/reprecipitation) plays an important role in the hydrothermal reactions, which transforms the irregular particles into regular nanocrystals. This result contributes to the further growth of nanocrystals at appropriate temperature[28]. Therefore, over-long reaction duration is not beneficial to the preparation of ultrafine particles, and 4.5 h is the optimal preparation duration.

2.2 Preparation of ultrafine tungsten carbide

2.2.1 Thermodynamic analysis and non-isothermal experiment

To investigate the feasibility of the carbothermal reduction of $PbWO_4$, thermodynamic calculations were conducted. Changes in the Gibbs free energy were used to determine the spontaneity of the reaction, and the initial reaction

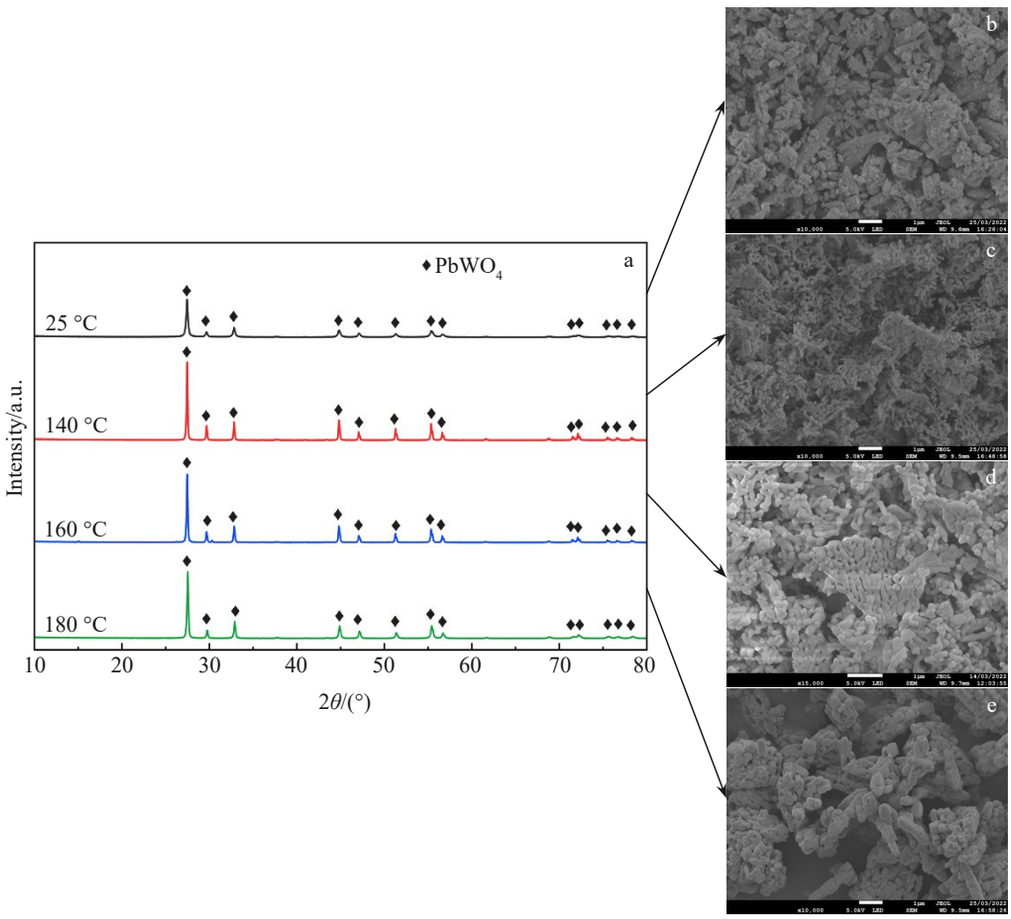

Fig.2 XRD patterns (a) and FE-SEM morphologies (b–e) of hydrothermal reaction products prepared at pH=7 and different temperatures for 4.5 h: (b) 25 °C, (c) 140 °C, (d) 160 °C, and (e) 180 °C

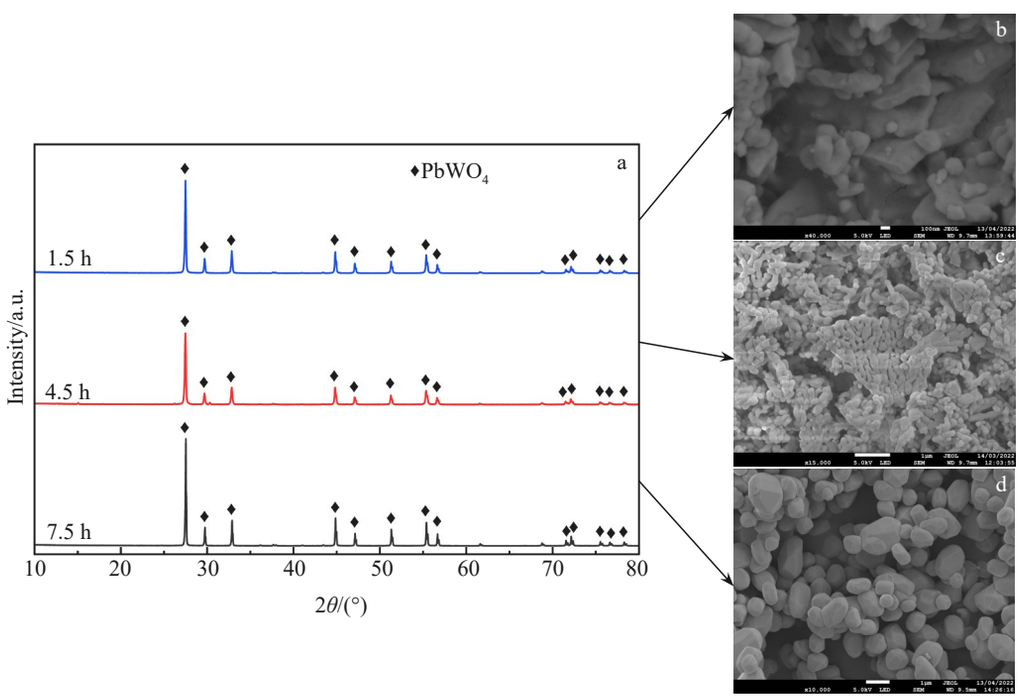

Fig.3 XRD patterns (a) and FE-SEM morphologies (b – d) of hydrothermal reaction products prepared at pH=7 and 160 °C for different durations: (b) 1.5 h, (c) 4 h, and (d) 7.5 h

temperature was determined with $\Delta G=0$[29]. The changes in ΔG with the reaction temperature ($\Delta G^{\ominus}_{T}$) are plotted in Fig. 4a. When the temperature is higher than 933 K (660 °C), $\Delta G^{\ominus}_{T}$ is negative, i. e., the reaction occurs spontaneously. However, due to the solid reaction kinetics of $PbWO_4$ and carbon black, the actual reaction temperature is higher than the calculated theoretical temperature.

Fig. 4b shows TG and DSC curves of the specimen with molar ratio of C: $PbWO_4$=5.5. According to TG curves (residual mass ratio), three inflection points appear at about 860, 940, and 1075 °C. The specimen shows a sharp mass loss from 860 °C to 940 °C, corresponding to the evaporation of CO_2, CO, and Pb from the specimen. From 940 °C to 1075 °C, the mass loss of specimen is mainly caused by the volatilization of CO and Pb vapor. When the temperature is higher than 1075 °C, the specimen undergoes slow mass loss, which mainly corresponds to the volatilization of Pb.

2.2.2 Carbothermic reduction process

Fig. 5 shows XRD patterns and FE-SEM morphologies of the carbothermic reduction products obtained under different conditions. As shown in Fig.5a, when the reaction temperature is 900 °C, the main phases are $PbWO_4$, Pb, WO_2, and W. When the reaction temperature increases to 950 °C, $PbWO_4$ and WO_2 disappear, indicating that this reaction temperature can completely eliminate $PbWO_4$. When the reaction temperature further increases to 1000 °C, the characteristic peaks of W disappear, and those of W_2C and WC appear. Generally, the lower temperature promotes the synthesis of products with fine particle sizes. Therefore, 950 °C is the optimal temperature for carbothermic reduction.

As shown in Fig. 5b, when the reaction duration is 1 h, the main phases are $PbWO_4$, Pb, and WO_2, suggesting that $PbWO_4$ cannot be sufficiently eliminated in such a short time. When the reaction duration is 3 h, the specimen consists of only Pb and W. When the reaction duration is 5 h, new phase W_2C appears, and the peak intensity of W decreases.

As shown in Fig. 5c, under molar ratio of C: $PbWO_4$=5, the main phase of specimen is W, and a small amount of WO_2 and Pb exists in the specimen. When the molar ratio of C: $PbWO_4$= 5.5, WO_2 phase disappears. When the molar ratio of C: $PbWO_4$ =6, new phase W_2C is generated. Therefore, increasing the molar ratio of C: $PbWO_4$ is beneficial to the carbothermal reduction process. Fig. 5d–5f show FE-SEM morphologies of carbothermic reduction products obtained under different molar ratios of C: $PbWO_4$. The carbothermal reduction products are mainly composed of particles with size of 55 nm. Under molar ratio of C: $PbWO_4$=5, blocky or rod-like particles can be observed in the product, possibly due to the aggregation of fine W particles, as shown in Fig. 5d. Fig. 5g shows FE-SEM image and corresponding EDS element distributions of carbothermic reduction product obtained under molar ratio of C: $PbWO_4$=5. It can be seen that the rod-like particles are mainly composed of W atoms and a few C atoms. However, in the fine particles, W and C elements are evenly distributed. This result indicates that the carbon black hinders the aggregation of fine tungsten powders and prevents the growth of ultrafine tungsten powders. Therefore, the large molar ratio of C: $PbWO_4$ is beneficial to obtain ultrafine products via carbothermic reduction.

2.2.3 Carburization process

To convert the carbothermic reduction products obtained at 950 °C for 3 h under different molar ratios of C: $PbWO_4$ to WC, the specimens were subsequently carburized at high temperatures. However, since the carbothermic reduction of $PbWO_4$ involves the evolution of CO_2, CO, and Pb vapor, many gaps are formed in the products, which impedes the growth of reduced W powder via the aggregation and sintering of small crystals. Additionally, W powder is not in full contact with the remaining carbon black, resulting in extremely slow carburization reaction between W powder and carbon black, i. e., incomplete carburization. Therefore, after the carbothermal reduction, the reduced products are mixed again for full contact between W powder and carbon black, which ameliorates the carburization kinetics.

Fig. 6 shows XRD patterns and FE-SEM morphologies of reaction products obtained under different carburizing conditions. In addition to WC, a small amount of W_2C can also be detected in the carburized products. Compared with the carbothermic reduction products, Pb and W disappear in the carburized products. Therefore, the volatilization of Pb

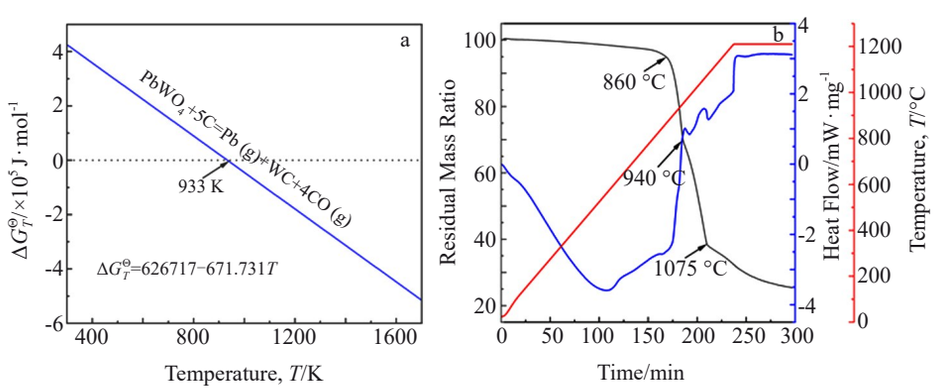

Fig.4 Thermodynamics of reduction and carburization process of $PbWO_4$ (a); TG, DSC, and temperature curves of reaction production during carbothermal reduction with molar ratio of C:$PbWO_4$=5.5 (b)

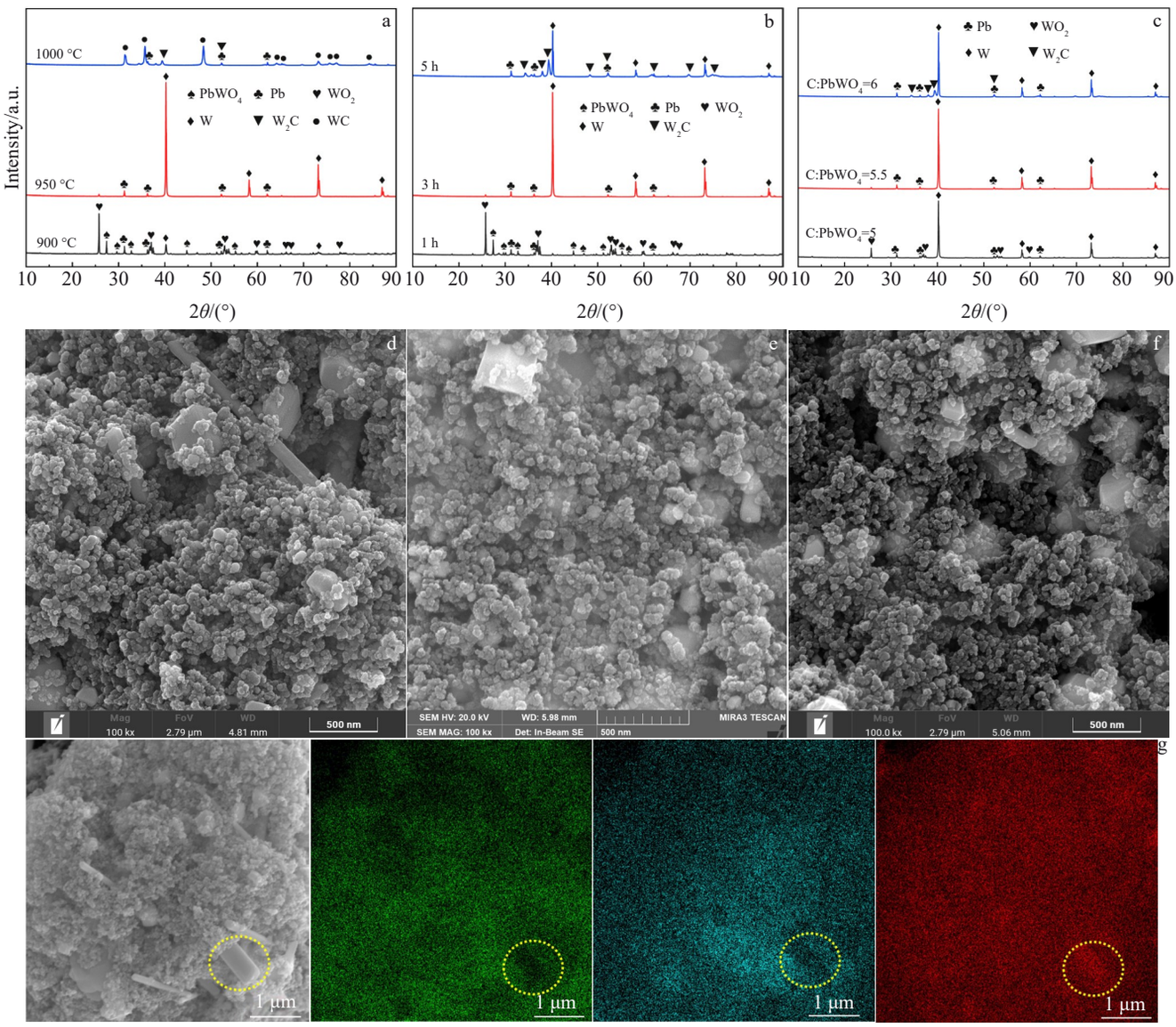

Fig.5 XRD patterns of carbothermic reaction products obtained under different reduction processes: (a) C:$PbWO_4$=5.5, 3 h, different temperatures; (b) 950 °C, C:$PbWO_4$=5.5, different durations; (c) 950 °C, 3 h, different molar ratios of C:$PbWO_4$; FE-SEM morphologies of carbothermic reduction products obtained under molar ratio of C:$PbWO_4$=5 (d), C:$PbWO_4$=5.5 (e), and C:$PbWO_4$=6 (f); FE-SEM image and corresponding EDS element distributions of carbothermic reduction product obtained under molar ratio of C:$PbWO_4$=5 (g)

from the products may result in the incomplete conversion of W_2C into WC.

Compared with that of the carbothermic products before reduction, the morphology of most particles does not obviously change. When C: $PbWO_4$=5 (theoretical value), most WC powder particles show irregular shapes and are connected to each other. The particle size is 60–150 nm. With increasing the molar ratio value of C:$PbWO_4$, more and more particles become smaller and have regular shapes. When molar ration of C:$PbWO_4$=5.5 and 6, the particle size is about 65 nm. TEM morphology of the WC particles prepared at 1200 °C after carburizing for 6 h under the molar ratio of C:$PbWO_4$=5.5 is shown in Fig. 7. It can be seen that the synthesized WC particles have regular shapes with average size of 60 nm. This result is in good agreement with that from Fig.6c.

The growth mechanism of WC powder during carbothermic reduction-carburization process is presented in Fig. 8a, which can be divided into two stages. The first stage is the reduction of $PbWO_4$ to W powder by carbon black. The second stage is the carburization of W powder. The first stage is crucial for the synthesis of ultrafine WC power, because the particle size of W powder significantly affects the final WC product. The industrial production of W powder is achieved by reducing WO_3 with hydrogen, which generates water vapor. As shown in Fig. 8b, tungsten oxides react with the water vapor to form volatile $WO_2(OH)_2$, and it is then reduced to W by H_2. W is deposited on the already-nucleated particles, resulting in the

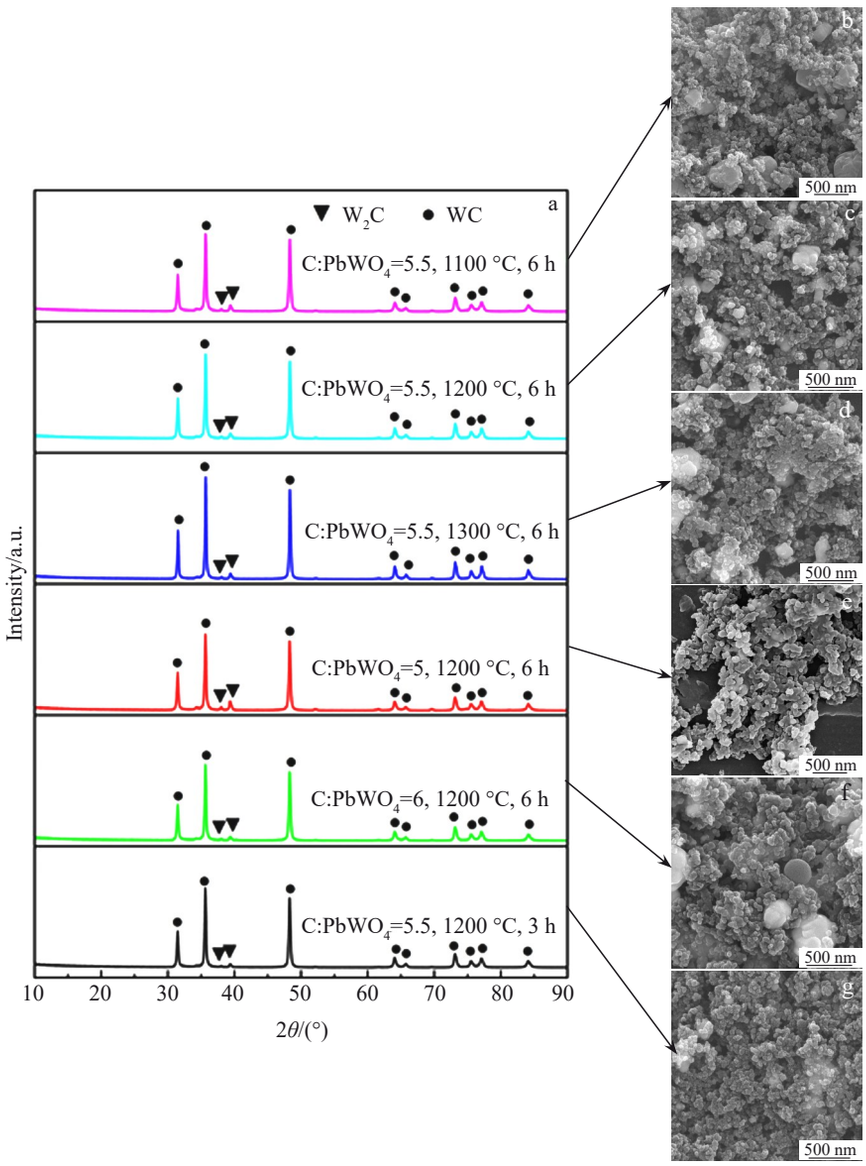

Fig.6 XRD patterns (a) and FE-SEM morphologies (b–g) of reaction products obtained under different carburizing conditions: (b) C:$PbWO_4$=5.5, 1100 °C, 6 h; (c) C:$PbWO_4$=5.5, 1200 °C, 6 h; (d) C:$PbWO_4$=5.5, 1300 °C, 6 h; (e) C:$PbWO_4$=5, 1200 °C, 6 h; (f) C:$PbWO_4$=6, 1200 °C, 6 h; (g) C:$PbWO_4$=5.5, 1200 °C, 3 h

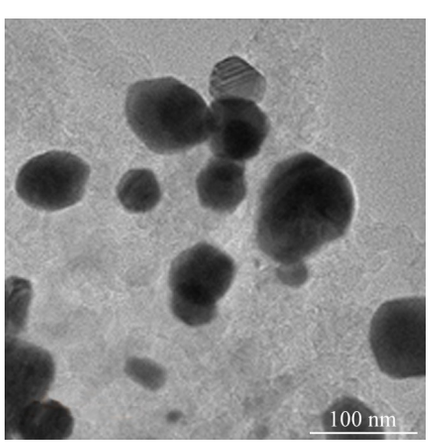

Fig.7 TEM morphology of WC particles prepared at 1200 °C after carburizing for 6 h under molar ratio of C:$PbWO_4$=5.5

formation of large W particles. However, according to Fig.8a, W powder can only be obtained by reducing $PbWO_4$ with carbon or CO during this stage, which hinders the growth of ultrafine W powder through the chemical vapor migration (CVT) mechanism. During the carbothermal reduction of $PbWO_4$, the volatilization of CO_2, CO, and Pb leads to many gaps between the products. Accordingly, due to the obstruction of these gaps and residual carbon black in the products, ultrafine W particles can hardly grow via aggregation. With increasing the molar ratio value of C:$PbWO_4$, more carbon black is trapped in the products, which can participate in the reduction reaction, resulting in the formation of more W nuclei. Nucleation and growth are usually the most critical steps in the preparation of ultrafine particles[30–31]. As a result, the W particles synthesized via the carbothermal reduction of $PbWO_4$ have ultrafine sizes. Afterwards, the

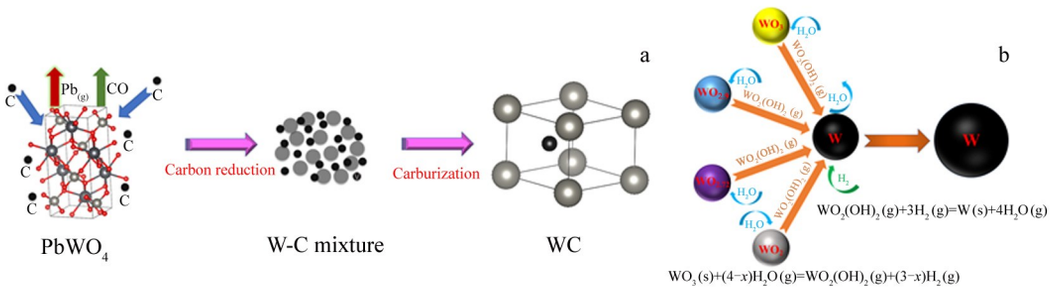

Fig.8 Schematic diagram of growth mechanism of WC powder during carbothermic reduction-carburization process (a) and CVT mechanism of W powder growth (b)

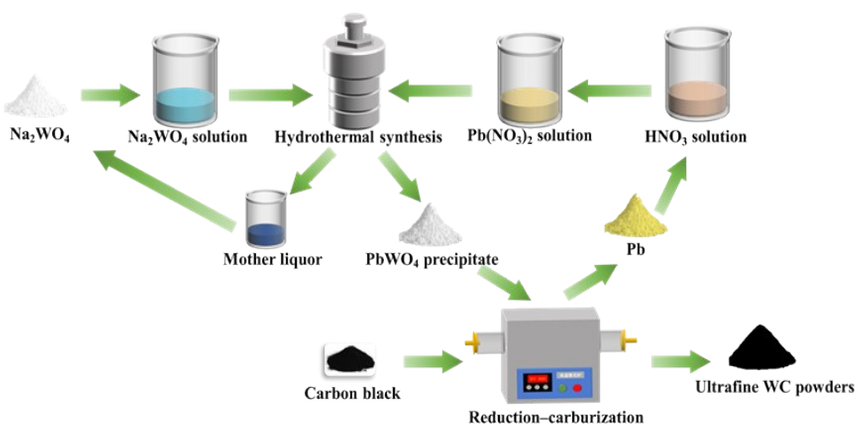

Fig.9 Schematic diagram of WC powder preparation process

reduction products are carburized at higher temperatures, W powder is converted into WC, and the remaining Pb is completely evaporated.

2.3 Flowchart of novel process to prepare ultrafine WC

Fig. 9 shows the process to prepare ultrafine WC powder using Na_2WO_4 as the raw material. Na_2WO_4 can be prepared during the main tungsten alkali metallurgical process. In this case, tungsten metallurgy and tungsten material preparation process can be combined to prepare ammonium paratungstate. This combined process also eliminates the ammonia nitrogen waste water, which is inevitably produced during the tungsten metallurgy. Due to the high vapor pressure of Pb, $PbWO_4$ can construct gas discharge channels, further decreasing the tungsten particle size during the carbothermal reduction. Pb can be recycled as an intermediate carrier for tungsten. As a result, $PbWO_4$ with average particle size of 0.4 μm can be prepared by hydrothermal method, and more than 99.9wt% of tungsten can be recycled.

3 Conclusions

1) $PbWO_4$ with average particle size of 0.4 μm can be prepared by hydrothermal method, and more than 99.9wt% of tungsten can be recycled.

2) Tungsten powder containing carbon can be obtained by reducing $PbWO_4$ at 950 °C for 3 h under the molar ratio of C:$PbWO_4$=5. Excess C can inhibit the agglomeration of tungsten powder, and the average particle size of tungsten powder is about 55 nm.

3) WC powder with average particle size of 60 nm can be obtained after the tungsten carbide powder is carbonized at 1200 °C for 6 h.

References

1 Ren H C, Li J T, Tang Z Y *et al*. *Journal of Cleaner Production*[J], 2020, 269: 122282
2 Li X K, Wang L, Liu Y *et al*. *Journal of Refractory Metals and Hard Materials*[J], 2023, 16: 106355
3 Tang Yanyuan, Zhong Zhiqiang, Chen Bangming *et al*. *Rare Metal Materials and Engineering*[J], 2023, 52(8): 2805 (in Chinese)
4 Zhang L W, Xi X L, Nie Z R *et al*. *Electrochemistry Communications*[J], 2022, 134: 107179
5 Wang X L, Song X Y, Liu X M *et al*. *Nanotechnology*[J], 2015, 26: 145705
6 Li J T, Luo Y J, Cui M Y *et al*. *International Journal of Refractory Metals and Hard Materials*[J], 2023, 113: 106212
7 Pan F, Liu J Y, Du Z *et al*. *CIESC Journal*[J], 2021, 72(11): 5455
8 Polini R, Palmieri E, Marcheselli G. *International Journal of Refractory Metals and Hard Materials*[J], 2015, 51: 289
9 Li J T, Cui M Y, Zhao Z W *et al*. *Hydrometallurgy*[J], 2022, 213:

105917
10 Li J T, Yang J H, Zhao Z W *et al*. *Minerals Engineering*[J], 2022, 181: 107462
11 Zhao Z W, Hu F, Hu Y J *et al*. *International Journal of Refractory Metals and Hard Materials*[J], 2010, 28: 633
12 Wang K F, Zhang G H. *Transactions of Nonferrous Metals Society of China*[J], 2020, 30(6): 1697
13 Pan F, Du Z, Li S F *et al*. *Chinese Journal of Chemical Engineering*[J], 2020, 28(3): 923
14 Liu Y K, Yang S N, Wang Z P *et al*. *Rare Metal Materials and Engineering*[J], 2022, 51(4): 1188
15 Wang Y, Long B F, Liu C Y *et al*. *High Temperature Materials and Processes*[J], 2021, 40(1): 171
16 Ostermann M, Dalbauer V, Schubert W D *et al*. *Tungsten*[J], 2021, 4: 60
17 Razavi M, Rahimipour M R, Yazdani-Rad R. *Journal of Alloys and Compounds*[J], 2021, 509: 6683
18 Wang K F, Chou K C, Zhang G H *et al*. *Advanced Powder Technology*[J], 2020, 31(5): 1940
19 Chen W H, Nayak P K, Lin H T *et al*. *International Journal of Refractory Metals and Hard Materials*[J], 2014, 47: 44
20 Dushik V V, Rozhanskii N V, Lifshits V O *et al*. *Materials Letters*[J], 2018, 228: 164
21 Wang K F, Jiao S Q, Chou K C *et al*. *International Journal of Refractory Metals and Hard Materials*[J], 2020, 86: 105118
22 Singla G, Singh K, Pandey O P. *Materials Chemistry and Physics*[J], 2017, 186: 19
23 La P Q, Ou Y J, Han S B *et al*. *Rare Metal Materials and Engineering*[J], 2016, 45(4): 852
24 Kim I, Park S W, Kim D W. *Nanoscale*[J], 2018, 10: 21123
25 Pervikov A V, Krinitcyn M G, Glazkova E A *et al*. *International Journal of Refractory Metals and Hard Materials*[J], 2022, 103: 105733
26 Guo S D, Shen T, Bao R *et al*. *Rare Metal Materials and Engineering*[J], 2018, 47(7): 1986
27 Wang K F, Zhang G H. *Transactions of Nonferrous Metals Society of China*[J], 2020, 30(6): 1697
28 Lin M, Fu Z Y, Tan H R *et al*. *Crystal Growth Design*[J], 2012, 12(6): 3296
29 Liu W B, Song X Y, Zhang J X *et al*. *Materials Chemistry Physics*[J], 2008, 109: 235
30 Wang K F, Sun G D, Wu Y D *et al*. *International Journal of Refractory Metals and Hard Materials*[J], 2019, 84(2–3): 104975
31 Sun G D, Zhang G H, Ji X P *et al*. *International Journal of Refractory Metals and Hard Materials*[J], 2019, 80: 11

水热合成钨前驱体-碳热还原-碳化制备超细纳米级碳化钨

李江涛[1,2]，罗勇进[1]，苏　淮[1,3]，赵中伟[1,2]，陈爱良[1]，刘旭恒[1]，何利华[1,2]，孙丰龙[1]，陈星宇[1,2]
(1. 中南大学 冶金与环境学院，湖南 长沙 410083)
(2. 稀有金属冶金与材料制备湖南省重点实验室，湖南 长沙 410083)
(3. 上海交通大学 材料科学与工程学院，上海 200240)

摘　要：提出了一种以水热合成的$PbWO_4$为原料，然后通过碳热还原-碳化获得超细WC的方法。以$PbWO_4$为钨中间产品，避免了氨氮试剂的引入；采用碳还原的方式可避免水蒸气的产生，抑制了钨粉的长大。结果表明：在初始pH为7.0、反应温度为160 ℃，反应时间为4.5 h的条件下，Na_2WO_4溶液中99.9%（质量分数）以上的W以$PbWO_4$的形式回收。然后采用低温碳还原$PbWO_4$，在C:W摩尔比为5、950 ℃的条件下还原3 h，获得了W和C的混合物，该混合物中预加富余的C有助于抑制钨粉的团聚。然后将W和C混合物高温碳化，在1200 ℃下反应6 h，获得了粒径约为60 nm的WC粉末。

关键词：钨酸铅；超细碳化钨；水热处理；还原碳化

作者简介：李江涛，男，1982年生，博士，副教授，中南大学冶金与环境学院，湖南 长沙 410083，电话：0731-88830476，E-mail：jiangtao-lee@csu.edu.cn